Section 4
LASER SYSTEM REPORT

4.A GDL Facility Report

Refurbishment of GDL continued during the fourth quarter of FY93. Activity concentrated on the installation of an imaging system to aid system alignment and the assembly of the second driver line that generates the so-called "foot" pulse.

The imaging system can acquire data from selected outputs of 17 video cameras located throughout the system, to one of five monitor pairs strategically located in the laser bay. The cameras view beamline centering and/or pointing at the ends of the various "legs" of the system. Dual monitors permit the operator to view simultaneously both centering and pointing images for a beam. Software-setable cross-hair references, beam cross-hair finding, and centroid-finding routines that operate at the 5-Hz repetition rate of the regenerative amplifiers are available. The imaging-system platform consists of a pair of 33-MHz 486 PC's that each contain two video frame grabbers and three LLE-designed-and-built, 5:1 (or 1:5) video multiplexers. Camera horizontal and vertical sync signals and frame-grabber trigger signals are derived from the laser's timing system to ensure proper synchronization of the image capture. Hand-held terminals located near the monitor pairs permit selection of the camera(s) to be viewed as well as selection of software routines. This system, along with new alignment sensor packages scheduled for installation in the first quarter of FY94, has and will ease alignment of the GDL system.

Significant progress was made in the installation, activation, and characterization of the foot-pulse driver line. This second driver line produces

the central beam of the co-propagated beam shape, which will also be used in the OMEGA Upgrade. The driver consists of a fiber-fed regenerative amplifier and a large-aperture ring amplifier (LARA). The system was activated in September. An energy and beam phase characterization was completed by the end of September and will be reported on in a future LLE Review article.

Simultaneous with the foot-driver-line activation, an annular apodizer was installed into the existing main-pulse driver line. Testing with this apodizer successfully produced the annular-shaped beam required for the main pulse. The outputs of the foot-pulse and main-pulse driver lines were merged on a beam combiner (a 45°-angle-of-incidence mirror with a central hole) to produce the first successful co-propagated beam. Work will continue in GDL during the first quarter of FY94 to propagate this beam shape through the system.

Finally, construction of the output end of the system continued during the fourth quarter. The system-output spatial filter was assembled, put under vacuum, and collimated. This spatial filter magnifies the clear aperture from 20 cm to 28 cm just prior to frequency conversion.

ACKNOWLEDGMENT

This work was supported by the U.S. Department of Energy Office of Inertial Confinement Fusion under Cooperative Agreement No. DE-FC03-92SF19460, the University of Rochester, and the New York State Energy Research and Development Authority. The support of DOE does not constitute an endorsement by DOE of the views expressed in this article.

4.B OMEGA Upgrade Status Report

Construction on the laser bay and target bay was completed by the end of August 1993, precisely on schedule. After taking occupancy of the building, LLE staff and contractors began the integration phase, which saw the first of the major structures entering the building for cleaning, alignment, and grouting into their exact final location on the laser bay floor. The stage-F alignment sensor package (FASP) structures, which are massive (30-ton) castings composed of a crushed granite and epoxy composite, have been placed in the target bay for imminent positioning and grouting.

The OMEGA Upgrade design is complete, as of 30 September 1993, and the final review documentation has been submitted to DOE. An Executive Summary has been provided, which contains a detailed overview of the complete system design. This issue of the LLE Review provides an excerpt from the Executive Summary, Sec. 5, which provides overviews of all of the major subsystems. Due to the length of this document, this issue will include subsystems from Laser Drivers through Amplifier Subsystems. Subsequent issues will include the remaining subsystem descriptions, such as Power Conditioning, Controls, Optomechanical Design and Major Structures.

Laser Drivers

1. Oscillators

The OMEGA Upgrade laser drivers comprise six synchronized oscillators: one continuous-wave (cw) mode-locked master oscillator; four regenerative amplifiers (regens); and one single-axial-mode (monomode), long-pulse oscillator. Extensive diagnosis and synchronous timing of these oscillators ensure the delivery of pulses with proper duration, precisely timed with respect to one another.

All oscillators and regens use crystals of Nd-doped yttrium lithium fluoride (Nd:YLF) as the active medium. The wavelength of this material matches well that of the phosphate glass amplifiers, and its material constants, particularly its gain and thermal properties, are ideally suited for oscillator applications. All oscillators and regens operate in a single transverse electromagnetic mode (TEM_{00}).

The master oscillator is a commercial cw mode-locked oscillator. This unit is a highly stabilized, actively mode-locked oscillator delivering a train of pulses of 80-ps duration at a rate of ~76 MHz. This oscillator operates in a thermally controlled environment and is extensively diagnosed to ensure stability. These diagnostics are discussed later in this article. The master oscillator provides the seed optical pulse to three regens: the main-, foot-, and short-pulse oscillators. Coupling between these oscillators is accomplished using optical fibers, ensuring flexibility and alignment insensitivity. In addition to providing the seed pulses (which define the timing of the shot event), the rf signal driving the mode locker is used as a reference for the electrical timing system. This timing system provides rates and timing fiducials for the portions of the laser system requiring timing to no better than 0.5 ns. Timing of events requiring higher precision (i.e., <0.5 ns) will be timed to this laser pulse using photodetectors. Triggering optical switches with the laser pulse provides a means to absolutely time events to the shot.

The need to frequency convert the OMEGA Upgrade laser to its third harmonic imposes the stringent requirement that each regen oscillator should operate with the same central wavelength. This need arises because each pulse (main and foot) will ultimately be frequency tripled by the same crystal and will require similar divergence, alignment, and wavelength. It is therefore necessary to monitor, control, and maintain a predetermined central wavelength for both oscillators. To limit the loss of main-pulse conversion efficiency to 0.5% the acceptable mismatch in wavelengths is ~0.2 Å. However, the implementation of SSD will require measurement of the central wavelength to <0.2 Å because spectral dispersion transforms frequency shifts to pointing shifts. To provide better wavelength stability the regens are fitted with temperature-stabilized etalons.

2. Regenerative Amplifiers

The first amplifiers for the main, foot, and short pulses are regens,[1–3] deriving their seed pulse from the master oscillator as indicated in Fig. 56.25. A single-mode, polarization-preserving optical fiber provides the link between the master oscillator and these regens. The regen cavity is a stable resonator operating in the

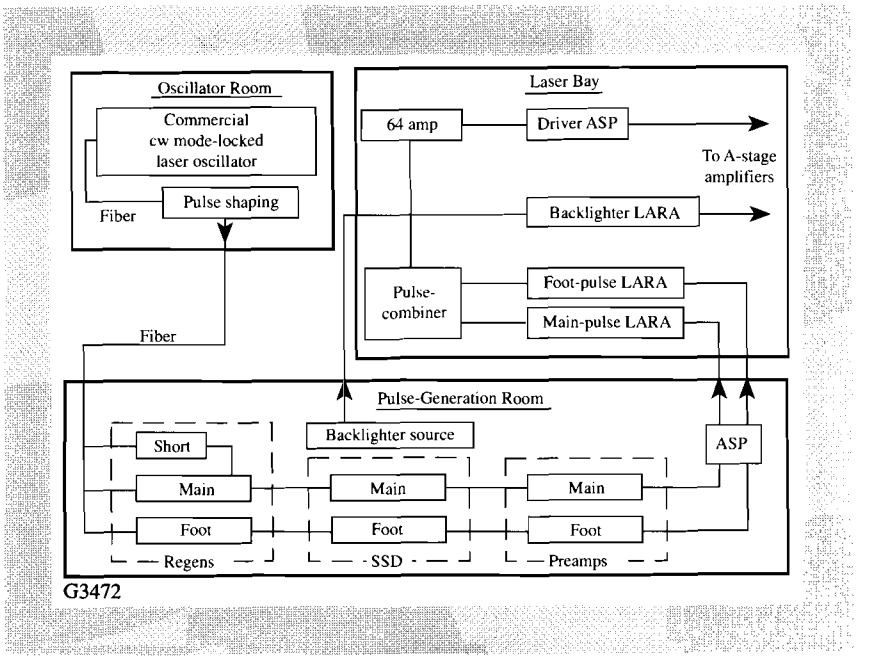

Fig. 56.25
A block diagram of the laser-driver subsystem, which comprises three separate areas: oscillator room, pulse-generation room, and the laser-bay driver line.

TEM_{oo} mode (Fig. 56.26). The duration of the pulses emitted by each regen depends on the intra-cavity etalons that temporally stretch the pulse as it circulates in the cavity. The short-pulse regen produces a pulse that can trigger electro-optical switches for truncation and pulse shaping. This requires <100-ps pulses, which are produced using no etalon in the cavity. The performance requirements for these regens are shown in Table 56.III.

For other future applications requiring pulses synchronized to the main laser pulse, it is possible to add more regens seeded by the master oscillator. This is planned for any optical probe beams that will be needed. These regens will be housed in areas remote from the laser driver rooms.

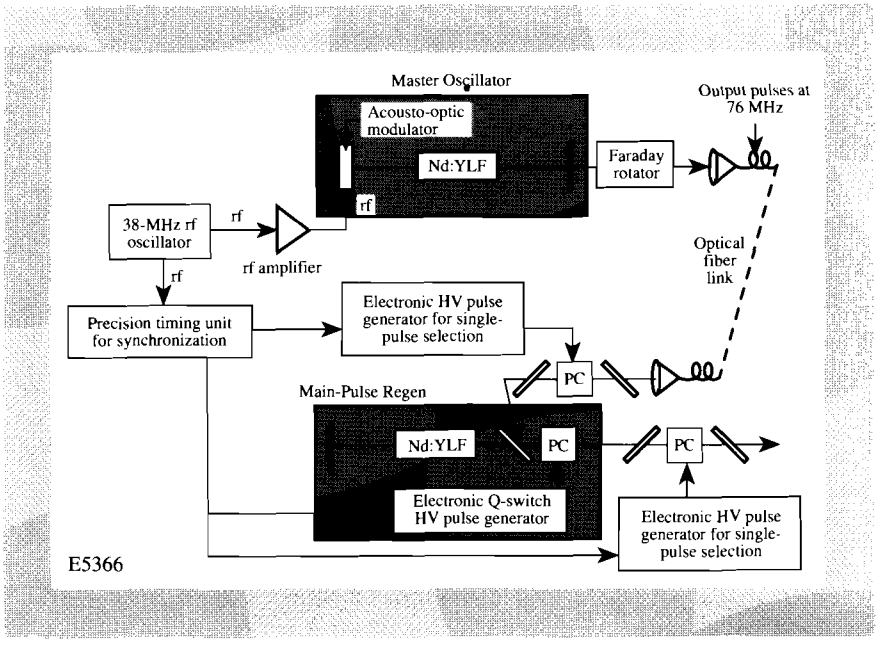

Fig. 56.26
The main-pulse regen is coupled (via an optical fiber) to the master oscillator. A similar configuration for the foot pulse ensures precise timing between the two pulses.

Table 56.III: Performance requirements of principal oscillators.

	Main-Pulse Oscillator	Foot-Pulse Oscillator	Short-Pulse[a] Oscillator
Seed pulse	cw mode-locked master oscillator		
Oscillator type	regen	regen	regen
Output energy (single pulse)	~1 mJ	~1 mJ	~1 mJ
Amplitude stability	≤2%	≤2%	≤2%
Pulse duration	0.5–1 ns	5–20 ns	0.1–1 ns
Temporal jitter between foot and main pulse	<30 ps	≤30 ps	≤30 ps
Pointing stability	≤10 μrad	≤10 μrad	≤10 μrad
Energy contrast (inter-pulse contrast)	>100,000:1	>100,000:1	>100,000:1

[a] This third regen is used for synchronized optoelectronic pulse shaping.

A fourth regen is used to amplify the backlighter pulse. This regen obtains its seed pulse from a long-pulse oscillator rather than from the master oscillator. The backlighter laser driver is discussed later. The use of a single (instead of multiple) master oscillator for all three oscillators was chosen to simplify synchronization of the many pulses generated. A layout of the regen table, which contains all of these oscillators, is shown in Fig. 56.27.

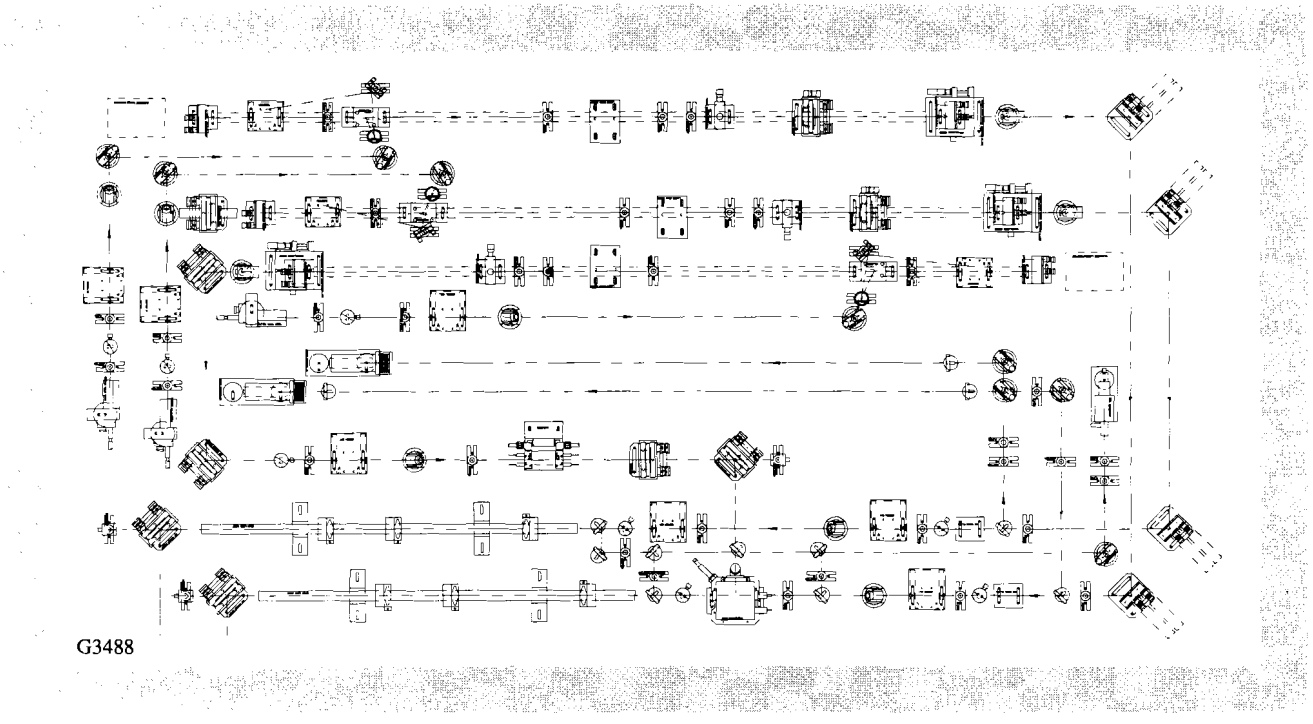

Fig 56.27
The regen table, in the pulse-generation room, has three (main-, foot-, and short-pulse) regens on it.

Reliable performance of regens requires high-contrast seeding, i.e., injection into the regen of a single pulse with high contrast. This is necessary since, in general, the cavity lengths of the master oscillator and the regens are not identical, and experience has shown that this leads to inter-pulse noise in the output pulse train from the regens. High contrast of the seed pulse is provided by an injection-isolation Pockels cell for each regen.

Synchronization of the master oscillator and the regen is provided by the pulse injected into the regen; the regen acts essentially as an optical delay line. However, the single-pulse switch-out in the injection path, the Q-switch in the regen, and the Pockels cell used for single-pulse selection following the regen must all be rigorously timed (phased) to the 38-MHz rf signal driving the acousto-optic mode-locker in the master oscillator. This is accomplished by the precision timing system mentioned later.

Amplitude stability of the single pulse selected for amplification in the main-pulse driver line is essential. This requires Q-switching of the regen under conditions of controllable and repeatable gain (population inversion) in the active medium. These conditions can be obtained from cw, quasi-cw, or pulsed operation of the Nd:YLF gain medium with adequate diagnosis. Further stabilization is achieved by using the intracavity intensity as feedback for control of the cavity losses. This control is implemented by the cavity Q-switch electronics.

3. Backlighter Source

In anticipation of x-ray backlighting experiments requiring a different type of laser pulse, provisions have been made to inject a third laser driver into 20 beamlines of the OMEGA Upgrade system. The source for this pulse consists of a single-axial-mode (monomode), long-pulse oscillator that seeds a regen similar to the others described earlier. This monomode oscillator produces a 20-ns pulse that is electro-optically chopped and then amplified by a regen. Synchronization of the self-injection-seeded monomode laser is accomplished through the timing of the cavity Q-switch and the electro-optic switch.

4. Synchronization of Oscillators and the Timing System

The requirement for synchronization of the various oscillators and electro-optical components is $\lesssim$30 ps. This is easily achieved because a single pulse is used to seed all of the regenerative amplifiers. The timing of the various electro-optical devices and electronic diagnostics is provided by the master timing system—a multicircuit system that generates both the rates and synchronization for the system. A block diagram of this system is shown in Fig. 56.28.

The master timing assembly is part of the laser drivers subsystem and will be located in the pulse-generation room. This unit will accept a master timing signal (nominally 38 MHz) from the master oscillator (optical) in the oscillator room. The rf mode-locked driver for this laser serves as the optical master oscillator for the OMEGA Upgrade. It will also accept two separate, hard-wired asynchronous "enable" signals from the power-conditioning host workstation and will be connected to an "inhibit loop" that links to other hardware and software devices.

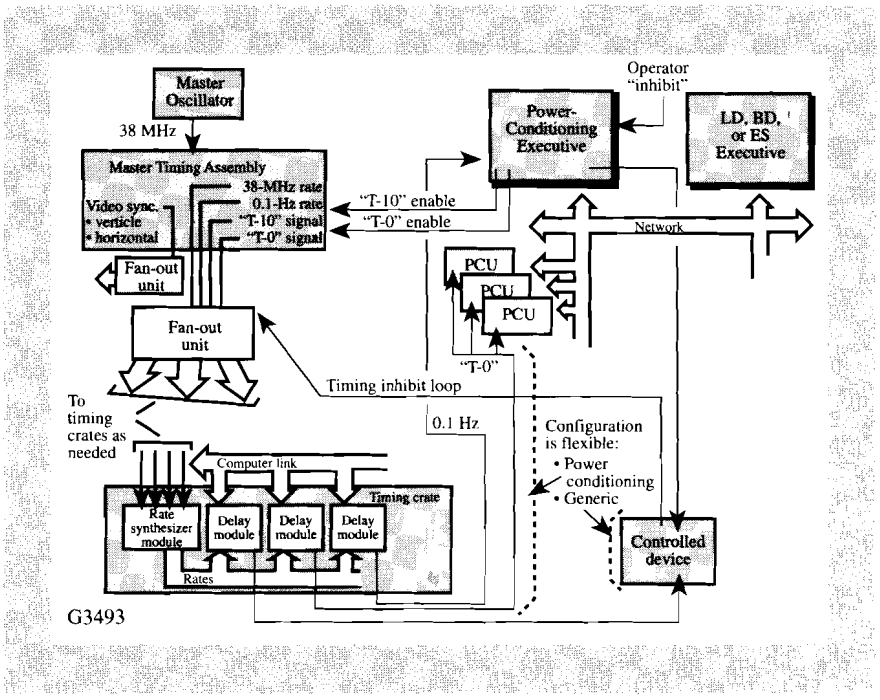

Fig. 56.28
The timing system is referenced to the 38-MHz rf signal that drives the master laser oscillator. Various slower rates are generated and distributed by this system.

The master timing assembly will output synchronized periodic timing signals and synchronized copies of the power-conditioning "enable" signals to associated "fan-out" boxes. The fan-out boxes will feed signals to the modular timing units. Fan-out boxes for video-synchronization, 38-MHz, and logic-level outputs are planned. The "inhibit loop" signal will be capable of interrupting all of these outputs.

The modular timing units will be located near the equipment they control and will provide a precisely delayed synchronous output signal of the appropriate voltage and duration. The synchronization rate source will be software selectable and will be based on the master timing assembly outputs. The output signal will be delayed relative to the input signal by a programmable value.

5. Smoothing by Spectral Dispersion (SSD)

Accommodations have been made for the implementation of SSD[4] in the laser driver. During the design of the PGR, the beam size and the optical layout were chosen to allow for the installation of the pre-delay gratings and the electro-optic modulator. In the laser-bay driver line, image planes were provided in the foot- and main-pulse optical systems to accommodate the placement of the angular dispersion gratings. Calculations were performed to determine the location of these gratings and the effect that their insertion will have on the placement of other optical components, namely alignment fiducials. To compensate for the insertion losses of the SSD components, preamplifiers have been added to the foot and main pulses.

6. Preamplifiers

The preamplifiers are small rod amplifiers that use conventional technology and are designed to operate at high repetition rates. The rods are high-quality ($\lambda/10$ @ 633 nm), 7-mm-diam Nd:YLF laser glass. The pump modules and

power conditioning are commercially available components. These amplifiers will be capable of operating at ~1 Hz with gains of ≥50. When used with the regenerative amplifiers, the output pulses will be of sufficient energy to facilitate real-time alignment and maintenance of the laser system.

7. Large-Aperture Ring Amplifier (LARA)

In traditional laser-driver configurations the final portion of the system staging is comprised of single-pass amplifiers; the number required is determined by the desired gain and output energy. By contrast, the Upgrade utilizes a single LARA for compactness and simplicity. This amplifier provides high gain (>20,000) and repeatable high-quality beams for pulses in the 0.1- to 10.0-ns range.

The LARA is a type of regenerative amplifier that uses a relatively large (40-mm) rod amplifier, a spatial filter, and an optical switch, all contained in an optical ring. Pulses are injected into the ring, circulate 3–4 round trips, and are switched out. During each round trip the pulse encounters an amplifier gain of about 14. This gain value is relatively conservative since a 40-mm amplifier can provide gains of 15–20 in this regime. This conservatism helps improve the reliability of the amplifier and provides ample reserve gain for future needs.

A schematic of the optical layout for the LARA is shown in Fig. 56.29. Central to its performance is the four-lens spatial filter that provides image relaying such that any location within the ring is mapped onto itself on subsequent round trips. This feature affords the ability to accurately align the ring and ensure that the optical path is reproducible, thereby allowing control of beam quality at high gain. The round-trip path length is approximately four times the effective focal length of each lens pair.

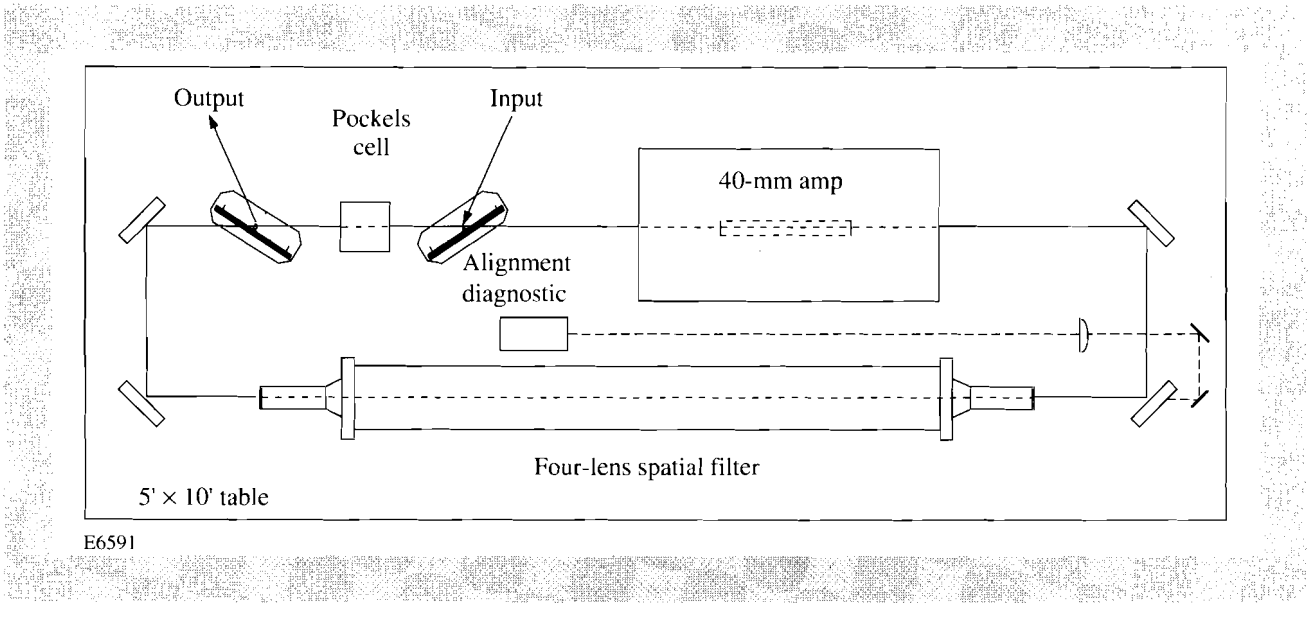

Fig. 56.29
The large-aperture ring amplifier (LARA) used in the OMEGA Upgrade laser driver. The Pockels cell admits the input pulse and then, after four round trips, switches the amplified pulse out. The four-lens spatial filter is used in defining the alignment axis.

The spatial filter pinhole is mounted to a pre-aligned position that serves as a pointing reference for alignment of the ring. The mount is kinematic so that the pinhole can be removed during fine alignment of cross hairs and accurately placed. The internal alignment of the LARA can be precisely maintained by aligning an intra-ring cross hair to itself and by aligning the beam to the spatial-filter pinhole using mirrors within the ring. An external beam is then injected into the ring and aligned to these references using external mirrors.

The injection and rejection (input and output) of pulses is performed using a Pockels cell and two polarizing beam splitters. Switching of the Pockels cell is driven by a thyratron-based switching circuit feeding a charge line; a switching time of much less than the cavity round trip time (22 ns) is achieved. The system will use a 66-ns charge line to provide four passes through the amplifier. The output prepulse contrast is better than 1000:1 and when followed by an isolation cell, a LARA can easily exceed the 10^5:1 contrast requirement.

The gain performance of the LARA versus the capacitor bank energy is shown in Fig. 56.30. Total gains of greater than 40,000 have been obtained with no appreciable degradation in beam quality (see Fig. 56.31). The design and performance of the LARA is presented in Ref. 5.

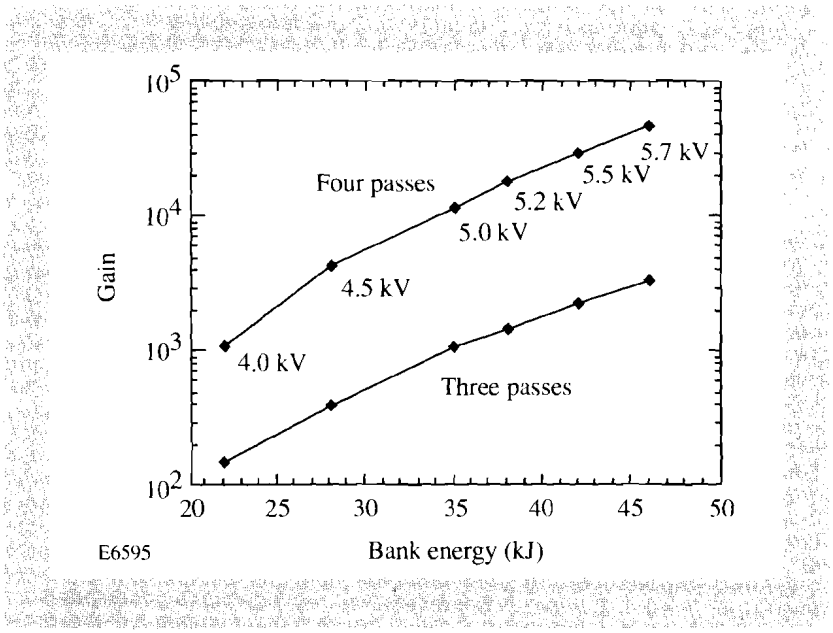

Fig. 56.30
The total gain of the LARA system as a function of capacitor bank energy. Gains greater than 10,000 are easily achieved with four passes through the ring.

8. Laser Driver Diagnostics

The propagated beam characteristics measured by the laser driver diagnostics can be divided into four categories:

(a) Energy
(b) Single-pulse and pulse-train-envelope FWHM
(c) Pockel cell timing jitter
(d) Spectral bandwidth and central wavelength through SSD

A laser driver's executive workstation host will collect data from these single-beamline diagnostics using the following measurement systems:

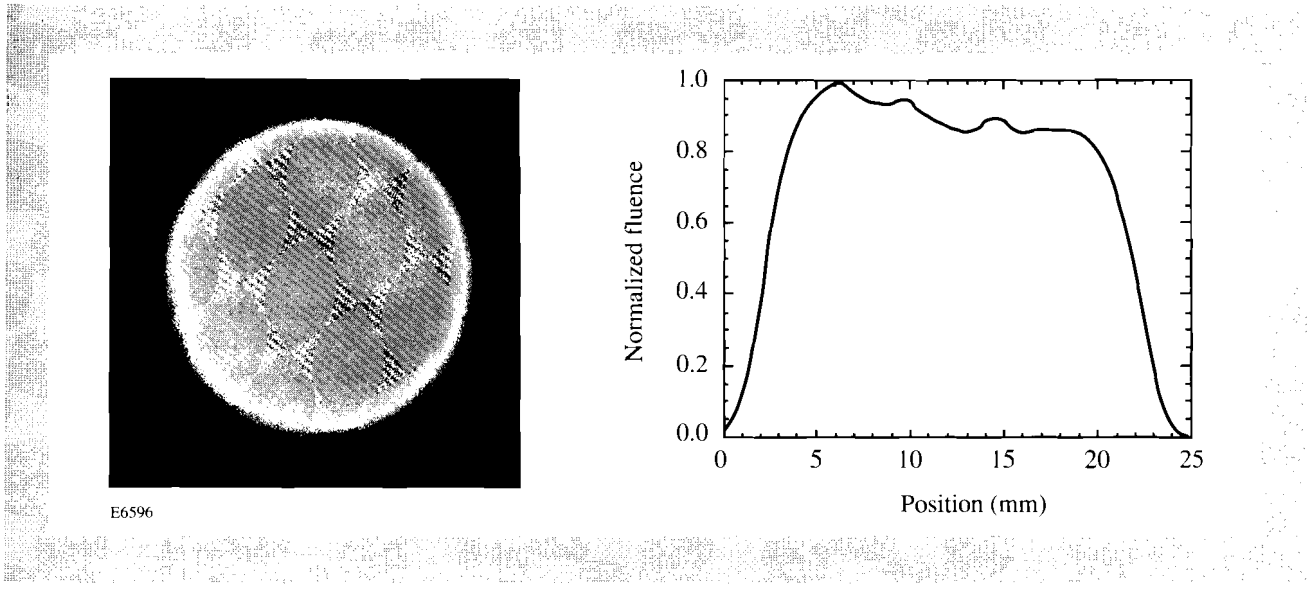

Fig. 56.31
The LARA output-beam image (and a lineout through it) for a 1-ns pulse with four round trips. The asymmetry in the intensity was caused by a misalignment of the input beam rather than by the performance of the LARA.

- Master oscillator monitoring and stabilization
- Regenerative amplifier (regen) characterization
- SSD (smoothing by spectral dispersion), laser-bandwidth broadening
- LARA characterization.

a. Laser-energy measurements. Energy measurements are made at several points along the laser drivers using photo-diodes that have been calibrated with a calorimeter. The charge created in each photodiode by the optical signal is integrated. The energy measurements are made at the 5-Hz cycle rate of the system, and real-time running statistics are computed from this data stream.

b. Single-pulse and pulse-train-envelope widths. The full width at half-maximum (FWHM) of both the single pulse and the cavity pulse-train envelopes are made at several key points within the system. The relatively slower, ~2-ms FWHM, pulse-train envelopes are sampled by standard photodiodes. The output signals are low-pass frequency filtered and captured by ~200-MHz digitizing oscilloscopes. These waveforms are read out of the oscilloscopes through their general-purpose-interface-bus (GPIB) communication ports, and the data are uploaded to the main diagnostic control computer for analysis. The much faster, ~1-ns FWHM, single pulses are sampled by fast vacuum photodiodes and high-bandwidth, ~5.0-GHz, transient digitizing oscilloscopes. In both cases, optimized communications and reduction software is used to meet the 5-Hz cycle rate of the laser system. Real-time running statistics are computed from this data stream and used to monitor the operational status of the system.

c. Pockels cell timing jitter. Pockels cells are used throughout the laser drivers to facilitate the operation of the system. The variation in the time delay between the origination of the Pockels cell trigger signal and the time when the full electric field appears across the cell is a key parameter that affects the pulse-to-pulse uniformity of the laser driver output. These timing variations, called "jitter," are of the order of ~1-ns high speed, 50 ps per count; time-to-digital converters

(TDC's) are used to make these jitter measurements. The TDC's use separate electrical input triggers to start and stop the internal counters. The start-counting trigger is derived from the master-timing fan-out, and the stop-counting trigger is generated by the electronics that drive the electric field on the Pockels cell. The number of counts within the TDC is read out, and the data are uploaded to the host computer for analysis. Real-time running statistics are computed from this data stream and used to monitor the operational status of the system.

d. Spectral bandwidth and central wavelength from SSD. The spatial intensity and phase uniformity of the laser beam are enhanced by using a technique based on SSD. This process is implemented within the laser drivers. The correct central wavelength and amount of bandwidth broadening of the laser after the SSD are important for high-efficiency, third-harmonic conversion. To monitor these parameters, spectral measurements are made to an accuracy of ±0.02 Å using a high-dispersion spectrometer. The detector coupled to the spectrometer output is a slow-scan, cryogenically cooled CCD array with 18 bits of dynamic range. The low quantum efficiency of the detector at 1 μm is overcome by efficiently coupling the light into the spectrometer (i.e., matching numerical apertures) and by sampling a high percentage (4%) of the laser-beam energy. The output of the array is buffered by an intermediate local controller and then passed along to the high-level diagnostic computer. This system is designed to operate at 1 Hz, collecting data on every fifth cycle of the laser. The spectrum of the pulse that is propagated for a full-system, high-power shot is always collected, independent of the 1-Hz acquisition rate. Real-time running statistics are computed from this data stream and used to monitor and adjust the SSD.

Laser Amplifiers

1. Amplifier Staging

The final aperture of the Upgrade was determined by the decision to use 60 beams (for high irradiation uniformity) and the requirement of 30 kJ of UV energy on the target. The beam size was then set by the damage threshold of the sol-gel coating on the input lens of the final spatial filter. The OMEGA Upgrade will have a final IR aperture of 20 cm, a substantial increase over the 9-cm aperture of the original OMEGA system.

a. Rod-amplifier staging. The rod-amplifier staging was dictated by the energy needed to compensate for the beam splitting required to generate 60 beams from a single driver line and, as with other designs, by budgetary considerations. The splitting, performed in steps of 3x, 5x, and 4x (actually two steps of 2x), in that order, was chosen (instead of, say, 10x and 6x) because of the availability of high-quality polarizer/splitters, with <6x splitting, using thin-film technology. This particular ordering was chosen because it produced a system configuration that fits inside the existing LLE laser bay. In addition, the splitting matches the saturated gain of the rod amplifiers to the energy partition. For example, the saturated gain of the rod amplifiers minus the losses in the beamline's applicable segment nearly equals the split fraction. This holds for the five-way split before stage B (6 cm) and the four-way split before stage D (9 cm). The three-way split was placed first because it minimizes the total number of rod amplifiers needed.

b. Power-amplifier staging. The final three amplifiers—a 9-cm rod, a 15-cm Brewster-disk amplifier, and a 20-cm disk amplifier—produce ~97% of the IR energy in each beamline. Moreover, nearly 90% of the system energy is in the main pulse, which has a temporal width in the range of 0.7 to 1.5 ns. The area ratios of the last stages are 1:2.78:5, a standard, short-pulse staging configuration entirely appropriate for the Upgrade's main-pulse performance. The penalty incurred for this staging is less-than-optimal performance for the foot pulse due to its longer pulse width (3–5 ns).

Several notable changes in staging have been made since the preliminary design. The original Galilean beam expander, between the 15- and 20-cm stages, has been changed to a standard spatial filter. This has the advantages of improving system longevity by filtering the beam, reducing the probability of optical ghosts, and easing the task of the optical system design by providing yet another image relay. Another important change having implications for system staging is a new baseline temporal pulse shape. The Title-I foot- and main-pulse shapes were essentially Gaussians (or for the foot, a Q-switched pulse shape). While these shapes will be used to initially validate system performance, ultimate operation will use newer, more complicated pulse shapes such as those shown in Fig. 56.32. Early fusion experiments will rely predominately on such pulse shapes.

For the continuous pulses the division between "foot" and "main" is more arbitrary than for the Gaussian pulses; this provides a level of flexibility in design. The frequency-conversion crystals now have a single thickness (instead of the "top-hat" design favored in the preliminary design) and are optimized for the main-pulse performance. The conversion-efficiency penalty incurred with the single-thickness crystals is mitigated by the freedom to change the area ratio of the foot and main pulses and also the temporal division between the pulses. Also, the additional cost and fabrication difficulty associated with top-hat crystals are avoided.

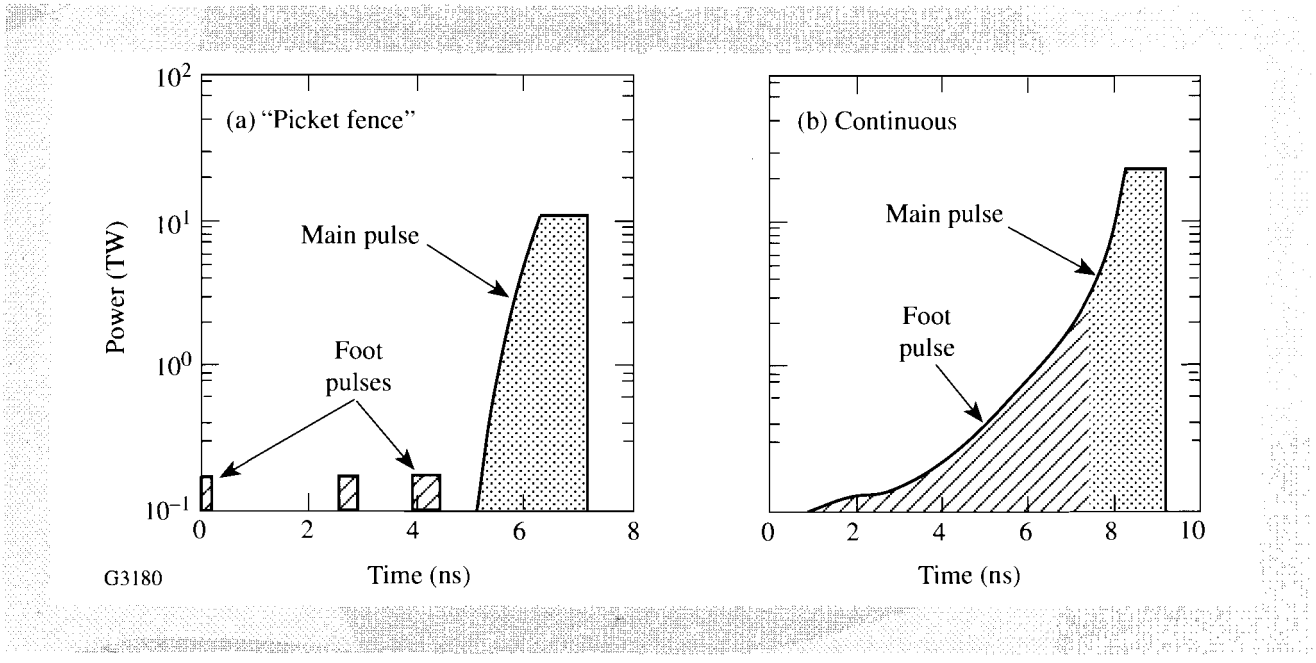

Fig. 56.32
Typical pulse shapes required for ignition-scaling experiments on the OMEGA Upgrade: (a) picket-fence pulse and (b) continuous pulse.

The B-integral is a measure of the phase retardation accumulated as a beam propagates through a medium possessing a nonlinear index of refraction. This phase retardation can cause self-focusing of optical noise in the beam, creating intensity modulations that can result in severe damage to a laser system. Spatial filtering removes these intensity modulations and essentially resets the wavefront distortion to an acceptable level. The laser designer is therefore concerned with the phase retardation accumulated between spatial filters, termed DB, which is typically kept below 2 rad. Moreover, practical constraints prohibit the complete elimination of phase retardation by the spatial filters. The resulting accumulation of residual retardation is termed SB. The effect of SB on laser performance is a complicated function of spatial frequencies and the estimates of optical noise in the system. The OMEGA Upgrade has SB's of 6.2 and 6.6 rad in the main and foot pulses, respectively, and no stage has a DB greater than 1.4 rad.

The energies, fluences, and B-integrals projected for the 39-TW version of the continuous pulse shape of Fig. 56.32 are shown in Figs 56.33 and 56.34. Typical of a medium-pulse-width (~1-ns) laser, the system performance is limited by damage fluence rather than by B-integral effects. It is expected that if DB rose to 2 rad, the nominal laser obscuration fractions (i.e., dirt) would yield a maximum spatial modulation of 1.8:1. Subsequent modeling has confirmed this expectation. All system fluences have been chosen such that the optical coatings can survive localized spikes in laser fluence 1.8 times higher than the average beam fluence. Recent experimental results indicate that if high cleanliness is maintained in the system, the 1.8:1 modulation is, indeed, conservative.

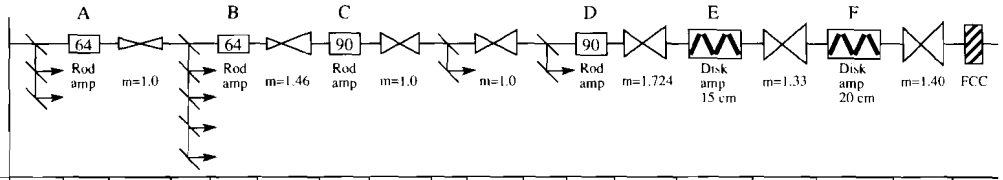

Clear aperture																		
Transmission																		
First photon gain																		
MAIN PULSE																		
Energy (J)	0.45	5.2	5.2	1.0	11	11	69	68	34	33	16	94	93	320	310	740	730	615
Avg. fluence (J/cm^2)	0.065	0.61	0.61	0.11	1.0	0.47	2.3	2.3	1.1	1.1	0.52	2.5	0.83	2.8	1.55	3.65	1.8	1.6
Sigma B (radians)	0.0	0.45	0.5	0.7	1.3	1.4	2.8	3.0	3.2	3.2	3.2	4.4	4.6	5.1	5.3	5.9	6.2	
Delta B (radians)	0.0	0.45	0.05	0.2	0.6	0.1	1.4	0.2	0.2	0.0	0.0	1.2	0.2	0.5	0.2	0.6	0.3	
FOOT PULSE																		
Energy (J)	0.54	4.0	4.0	0.75	5.4	5.3	22	22	11	10	5.1	21.5	21	70	69	160	160	82
Avg. fluence (J/cm^2)	0.18	1.3	1.3	0.24	1.7	0.79	3.2	3.2	1.6	1.5	0.72	2.9	1.1	3.4	1.9	4.3	2.1	1.2
Sigma B (radians)	0.1	0.9	0.9	1.25	2.1	2.3	3.7	3.9	4.1	4.1	4.1	5.1	5.2	5.3	5.9	6.4	6.6	
Delta B (radians)	0.1	0.8	0.0	0.35	0.85	0.2	1.4	0.2	0.2	0.0	0.0	1.0	0.1	0.1	0.6	0.5	0.2	

Fig. 56.33
Energy, fluence, ΣB and ΔB from the A amplifiers to the FCC's, for the main and foot pulses (39-TW continuous pulse shape).

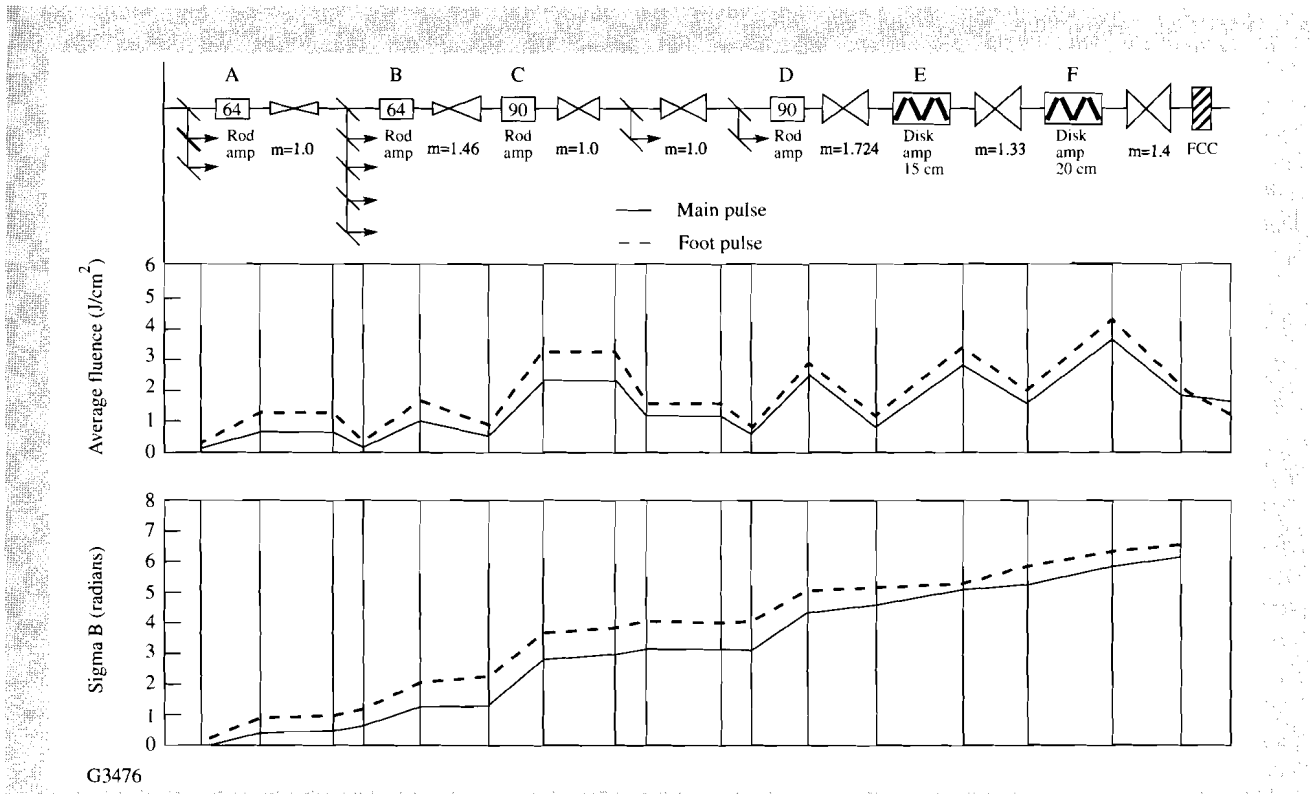

Fig. 56.34
Fluence and cumulative B-integral from the A amplifiers to the FCC's for the main and foot pulses (39-TW continuous pulse shape).

2. Rod Amplifiers

The ninety-four 64-mm and 90-mm rod amplifiers needed for the OMEGA Upgrade system will be fabricated from a design that reuses parts of the 54 amplifiers from the OMEGA system. Refinements to the original design have been implemented as a result of 12 years of experience using these amplifiers, and are aimed at improving performance, serviceability, and conformity to the rest of the system. The rod amplifier consists of a frame, a rod module, a pump module, and the various electrical and fluid connections. The rod-amplifier assembly is shown in Fig. 56.35.

The rod-amplifier frame is unchanged from the original design. The rod module has been redesigned to reduce the number of parts in order to cut cost and improve serviceability. The material used for all parts has been changed to improve resistance to corrosion by the deionized water/ethelyne glycol solution used to cool the rods. The flow pattern for this coolant has been improved to provide more-uniform heat extraction, thereby reducing thermal stress in the rod.

The pump module, containing the flash lamps and reflectors, will utilize the same external shell, but the reflectors and flash-lamp assemblies have been changed. A new reflector configuration, a simple searchlight reflector geometry designed using the ZAP Monte Carlo ray-trace code,[6] has been implemented to improve the cavity transfer efficiency. Prototype testing of this module will demonstrate the amount of increased performance of this design. The rod amplifiers use a 305-mm-arc-length, 300-Torr xenon flash lamp and the same connectors as used on the disk-amplifier pump modules. The flash-lamp assemblies

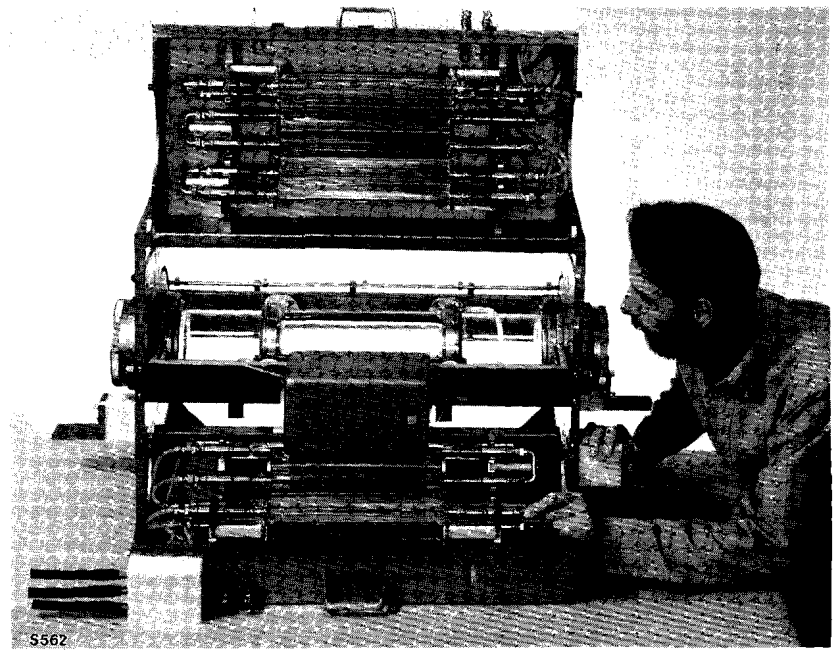

Fig. 56.35
The OMEGA-style rod amplifier used in the Upgrade. The pump modules (top and bottom) are open, showing the flash-lamp assemblies. These will be modified slightly to improve performance; the rod yoke assembly will be modified to improve reliability.

have also been redesigned to incorporate a configuration similar to the disk-amplifier bricks. The high-voltage connectors for the amplifier are to be identical to the ones used for the disk amplifiers.

The laser glass rods have been extended to 370 mm in length to accommodate improved O-ring seals. It was found that if the ends of the 90-mm rods were made parallel, an internal, end-to-end reflection would propagate unwanted energy just outside the laser aperture. To inhibit this reflection, the 90-mm rods will be finished with a 0.6-mrad wedge that prevents retroreflection within the rod.

3. Disk Amplifiers

The amplifiers for stages E and F are modern, 15- and 20-cm clear aperture, Nd:glass Brewster-disk amplifiers. The amplifiers are termed modern because they incorporate several unique features as well as a number of improvements suggested by others[7] who have extensive experience in building disk amplifiers. These improvements include minimization of total amplifier volume[8] for better coupling of pump light to the laser glass, transversely pumped rectangular design to avoid obscuration of flash lamps by disk supports,[9] water-cooled flash lamps,[10] and polymerically bonded edge cladding.[11]

Each amplifier contains four Nd:phosphate glass (3-wt% doping), 3-cm-thick disks.[12] The number of disks was chosen to obtain adequate gain using the 3-cm-thick disks—a thickness chosen to minimize the B-integral. The pump pulse width was then optimized $\left(3\sqrt{LC} = 550\,\mu s\right)$ for high gain per unit path in the disks. Pump radiation is supplied by 19-mm-bore, water-cooled xenon flash lamps mounted on either side of the cavity.

Since the majority of the laser energy is in the relatively short (~1-ns) main pulse, an optimization of focusable power per amplifier dollar was more appropriate than total stored energy per amplifier dollar. The results of this optimization, plus a wavefront budget analysis for the system, yielded the

optical requirements for the 20- and 15-cm amplifiers that are summarized in Table 56.IV.

These requirements impose constraints on the mechanical and electrical design of the amplifier. As an example, the gain requirement results in pump-light fluences capable of incinerating any contamination within the amplifier. Since this could result in possible damage to the laser disks, high levels of cleanliness are required; these constraints are summarized in Tables 56.V and 56.VI.

A consistent and well-reasoned design philosophy is essential to meet all performance requirements and maintain safe design. To effect this, the philosophy addresses three aspects of the design: reliability, maintainability, and producibility.

The amplifiers have been designed for a 15-year, 20,000-shot lifetime. Reliability is driven by a number of factors such as system lifetime, maintenance intervals, and gain stability. Assuming one of the 120 disk amplifiers is maintained each week, the maintenance interval will be approximately 2.5 years. The degradation of the amplifier optical performance during this interval must be minimal.

Maintenance of the disk amplifiers has been approached in three ways: First, the amplifier must require minimal maintenance. Second, the most probable maintenance tasks (e.g., flash-lamp replacement) must be performed in place and be completed within a 60-min shot cycle. To facilitate this, the tools required must be minimal. Amplifiers are removed only for full maintenance or catastrophic failure. Third, repairs on subassemblies are conducted off-line, i.e., new assemblies are swapped in and the old ones repaired off-line.

Table 56.IV: Amplifier-performance optical requirements.

Clear aperture in centimeters	15	20
Number of disks per amplifier	4	4
Thickness per disk in centimeters	3.0	3.0
First-photon center-line gain	4.2	3.0
Gain uniformity across aperture	±10%	±10%
Average stored-energy density in J/cm^3 (assuming a stimulated emission cross section of 3.5×10^{-20} cm^2)	0.54	0.41
Cavity transfer efficiency	>1.14%	>1.14%
Nd_2O_3 doping in wt%	3.0	3.0
$3\sqrt{LC}$ pump-pulse width, microseconds	550	550
Passive transmission	>96%	>96%
Wavefront, waves rms at 1054 nm	1	1
Repetition rate, shots per hour	1	1

Table 56.V: Mechanical requirements.

- Only organics that can survive intense UV irradiation
- Disk cavity isolated from the external environment
- Nitrogen purge for disk and pump cavities
- Maintainable on a 1-h shot cycle
- Class-100 compatibility a minimum, Class 10 a goal
  - permissible cleaning techniques
  - ultrasonic bath
  - high-pressure Freon or water spray
  - solvent wipe

Table 56.VI: Electrical requirements.

- Negligible contribution to 120-mΩ resistance budget of pulse-forming networks
- Materials compatible with deionized (18 MΩ•cm) water
- 40-kV dc standoff
- Electrically insulated in case of fault
- Provide ground plane for flash lamps

To ensure the amplifiers are produced in a cost-effective manner, considerable manufacturing engineering has been incorporated into the amplifier design. Conventional manufacturing methods that permit mass production have been used in addition to purchased parts whenever possible.

The 15- and 20-cm amplifiers consist of four major subassemblies: pump modules, flash-lamp bricks, disk-frame assemblies, and the amplifier-frame assembly. The 20-cm disk amplifier is depicted in Fig. 56.36. The amplifier frame supports the various other subassemblies. Hinged to the side of this frame are the pump modules that house the flash lamps and serve as the outer face of the optical cavity. The laser glass disks are mounted in disk-frame assemblies within the amplifier frame.

a. Amplifier-frame assembly. The frame assembly consists of seven major components that form the structural backbone of the amplifier. All components are machined from solid pieces of 6061-T6 aluminum, stress relieved and electroless nickel plated. The plating prevents oxidation and seals the exposed surfaces for operation in a class-100 clean area.

The amplifier frame design is nearly identical (except for scale) for the 15- and 20-cm amplifiers. The disk-frame assemblies kinematically mount within the frame assembly to avoid inducing stresses in the disk. The pump modules are held flush against the frame by spring-loaded hinges to minimize light leaks. Inside the frame the top, bottom, and ends of the optical cavity are constructed of separate, highly polished, silver-plated reflectors to maximize cavity transfer efficiency. The pump modules form the sides of the cavity and are separated from the laser glass by 6-mm-thick blast windows.

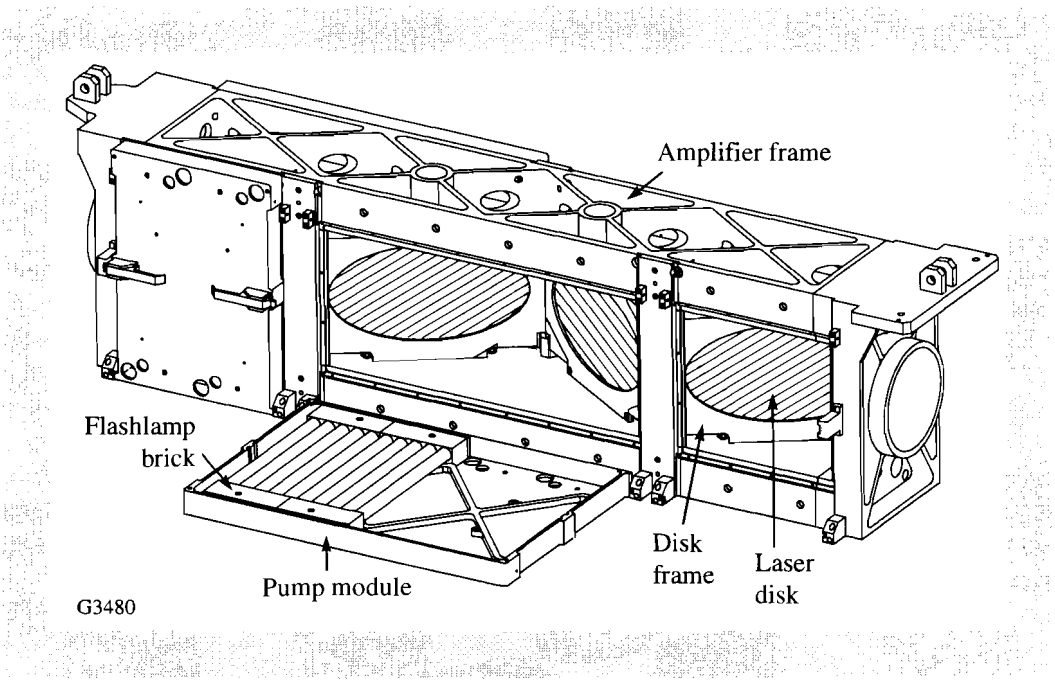

Fig. 56.36
The major components of the 20-cm disk amplifier for the OMEGA Upgrade. The 15-cm disk amplifier is a similar configuration (albeit smaller) but has longitudinal flash lamps rather than transverse.

Blast windows serve two functions in the amplifier design, which require class-100 clean-room conditions. First, they provide isolation from the class-1000 laser bay environment when the amplifier is opened for servicing. Secondly, the blast windows stop flash-lamp-generated acoustic disturbances that would degrade the transmitted wavefront quality.

b. Pump-module assemblies. The pump modules containing the flash-lamp bricks and reflectors have been specifically designed to permit *in-situ* replacement of flash-lamp-brick assemblies. A novel mechanical design with quick-release electrical and coolant connectors allows the replacement of a flash-lamp brick within the required 1-h shot cycle.

To maximize the cavity transfer efficiency the pump modules contain a highly polished, silver-plated, flat reflector placed within 1 mm of the flash-lamp water jacket. The proximity of this reflector provides the electrical ground plane essential for flash-lamp triggering. To prevent degradation of the silver surfaces, the pump modules are kept in a slightly pressured (<1-psi) nitrogen environment. As a secondary feature, the nitrogen environment reduces acoustic noise generation from the absorption of the lamp light in Schumann-Runge bands in oxygen between 175–195 nm.[13]

c. Flash-lamp-brick assembly. The disk amplifiers are pumped by (12) 1.32-m-arc-length or (80) 0.25-m-arc-length, 19-mm-bore, water-cooled xenon flash lamps. The flash lamps are mounted on 34-mm centers for a packing fraction of 1.75. The flash lamps are driven by (12) or (16) 19-kJ pulse-forming networks (PFN's). This results in total bank energies of 227 and 300 kJ at nominal bank voltage with the lamps operating at a 26% explosion fraction. These bank energies are based on 1.14% cavity transfer efficiency. The pulsed-power system also includes a pre-ionization lamp check (PILC).[14] (See **Power Conditioning** in the next issue of the LLE Review.)

The flash-lamp-brick assembly consists of a flash lamp or group of flash lamps, their water jackets, the electrical connections, and water connections. For the 15-cm amplifier, a brick consists of a single flash-lamp assembly. Five flash-lamp assemblies are used in a brick for the 20-cm amplifier. In both cases, the total flash-lamp arc length is about 1.3 m. The five flash-lamp assemblies are connected in series electrically and for coolant flow.

Cooling with deionized (DI) water has a number of advantages. The DI water used in the closed-loop cooling system has a resistivity of 10–18 MΩ•cm. At this resistivity level the DI water serves as an electrical insulator.[15] Water cooling has been demonstrated to improve flash-lamp reliability, especially when lamps are operated at higher fractions (20%–35%) of explosion energies. As opposed to air-cooled flash lamps, which fail in an explosive manner depositing glass and metallic debris over a large area, water-cooled flash lamps fail in a noncatastrophic manner—they simply fill with water. A catastrophic failure that generates debris is not acceptable for amplifiers operating in a class-100 environment.

Each flash-lamp assembly consists of a flash lamp, a water jacket, and two flash-lamp connectors. The flash-lamp assemblies are 300-Torr xenon flash lamps of either 1.3-m or 0.25-m arc length. To reduce UV emission, the flash-lamp envelopes (22 × 1.5-mm tubes) are made of cerium-doped quartz (CDQ). Because metallic ions are highly soluble in DI water, the flash-lamp lugs are passivated 316 stainless steel. In addition, all components of the flash-lamp connector directly exposed to DI water are also made of 316 stainless steel. The remaining components of the flash-lamp connector are made of 20%-glass-reinforced Ultem[16] to provide electrical insulation. The water jackets are made from 27 × 1.5-mm Corning[17] 7740 Pyrex tubing.

d. Disk-frame assemblies. Except for scale, the disk frames of the 15- and 20-cm amplifiers are identical. Each assembly has two pieces (frame and cover) machined from solid plates of 6061-T6 aluminum, stress relieved and silver plated. Care is taken to center the laser disks within the frame and to ensure a 5.1-psi, "continuous" elliptical ring contact on the laser glass surface. The metal-to-glass contact area never overlaps the laser glass to cladding glass bond line. Modeling of this design has shown that the induced Hertzian stresses[18] decay outside the disk's clear aperture.

4. Amplifier Performance

In the upgraded system, 97% of the IR energy is produced after the last split, in the last three amplifiers. Because of the importance of this portion of the system and the relative ease of prototyping a simple chain without splits, a replica of this chain was constructed and its large-signal performance evaluated. These tests were conducted after an extensive series of small-signal measurements were performed on the disk amplifiers. The small-signal data so accumulated were necessary to compare the large-signal data to theory. Detailed comparisons between theory and experiment could then be made via simple Frantz-Nodvik models.[19] The small-signal characterizations[20] will not be described here, but the results of these tests will be used freely to explain the large-signal results.

The large-signal performance was evaluated under specific conditions that

took advantage of existing drivers and eased interpretation of the results. The first condition was that the test beam was not co-propagated. In the final amplifier the aperture was filled with an 18-cm single beam. The temporal pulse shape was nominally a 740-ps-wide Gaussian from the mode-locked oscillator. Since advanced uniformity schemes require various types of modulation, testing was performed with transform-limited, 740-ps pulses, FM-modulated pulses with 5 Å of bandwidth and, finally, with spectrally dispersed, FM-modulated pulses used in the SSD scheme. The measurements included output energy versus input energy on a stage-by-stage basis, the passive losses per stage, and the near-field beam quality.

The test beamline is schematically shown in Fig. 56.37. A beam from the then-existing OMEGA system was picked off and injected into the prototype 15- and 20-cm amplifiers. A prototype of the spatial filter to be used on the Upgrade between stages E and F was placed between the amplifiers. Since a similar prototype of the Upgrade's output spatial filter was not available, a 21-cm-clear-aperture $f/14$ spatial filter (from LLNL) was used at the output. The acceptance angle of that final filter was chosen to be 800 mrad, half-width. This was primarily driven by pinhole closure considerations.[21]

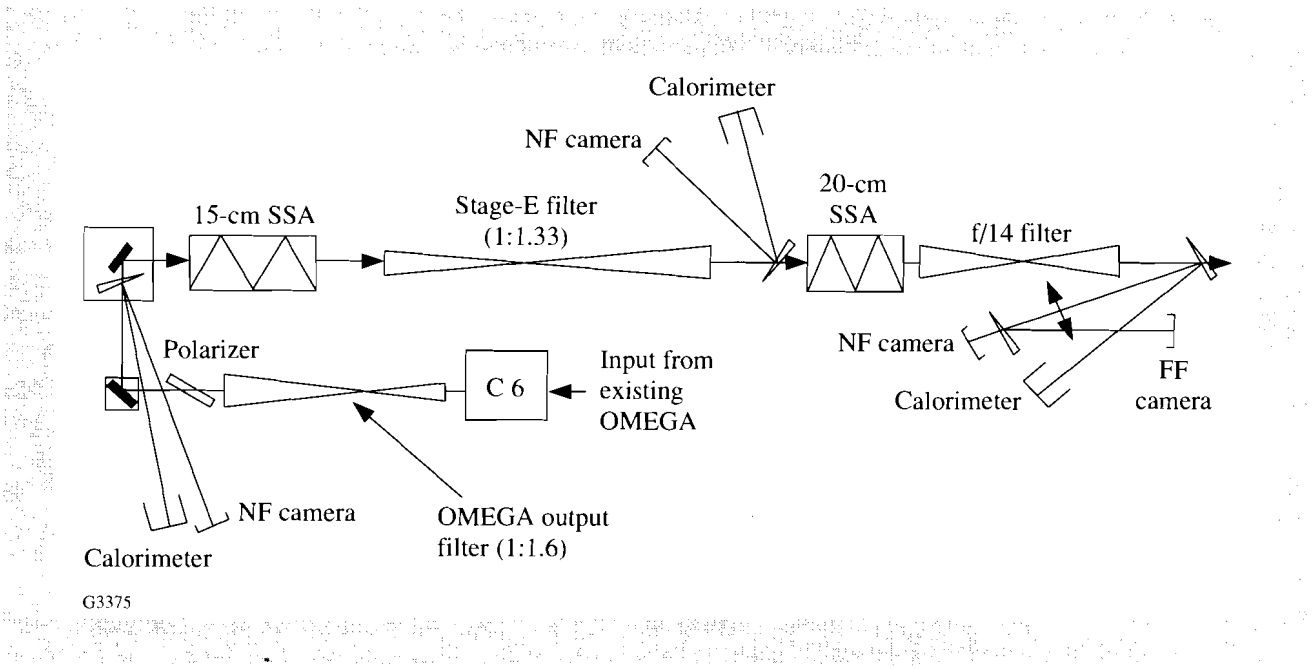

Fig. 56.37
The experimental setup for the demonstration of 1 kJ out of a single Upgrade beamline. The input was the 90-mm output of the original OMEGA system. Note that all diagnostics are after the spatial filters to insure measurement of only focusable energy.

The results of these tests are presented in Fig. 56.38, a plot of energy out of the test beamline for both 15- and 20-cm amplifiers versus drive energy from the 9-cm rod amplifier. The measurements were taken after a spatial filter to ensure that only focusable energy was measured. The Upgrade design goal is equivalent, in this simplified configuration, to a 1.0-kJ output with 140-J input; this was readily achieved. Also shown in Fig. 56.38 are the predictions of a simple Frantz-Nodvik[19] calculation of the large-signal gain. In order to perform this calculation, the saturation fluence, small-signal gain, passive losses, and beam profiles were required. [Published values of the saturation fluence were used (nominal 3.75 J/cm^2) with the two-ion model of Yarema and Milam.[22]] Stage-

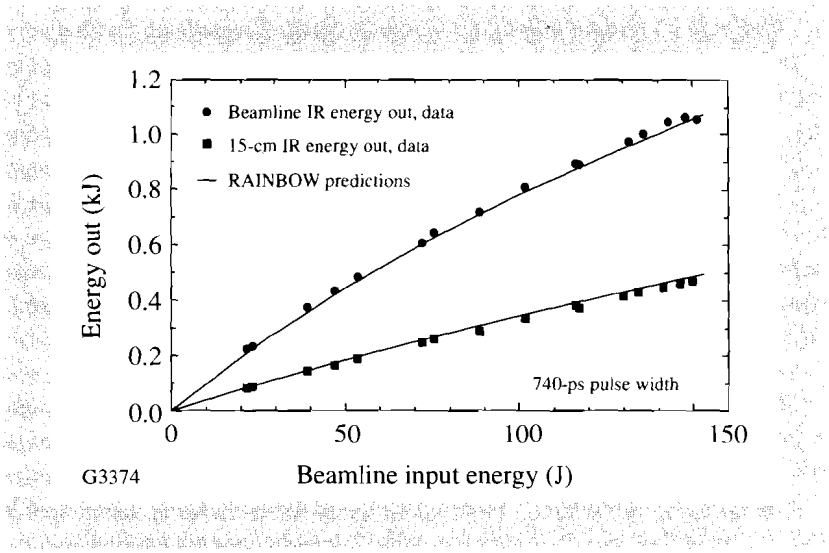

Fig. 56.38
The output energy of the beamline shown in Fig. 56.37 versus input energy. The goal of 1 kJ was reached at ~150-J input, thus assuring the energy performance of the OMEGA Upgrade.

by-stage passive losses were measured calorimetrically with the amplifiers unpumped. The beam profile was measured by taking near-field photographs on high-speed IR film and converting density to intensity. Small-signal gain was measured during the separate off-line characterization of each of the amplifiers; reasonable agreement was observed.

In addition to the energy-transport measurements, targeting-stability concerns dictated that a full-aperture, pointing-stability characterization be performed. In this measurement, the two disk-amplifier stages were double-passed by a full-aperture, Q-switched Nd:YAG beam. The double-passing was accomplished by placing a partially reflecting mirror at the output of the chain. The outgoing and return beams were imaged onto a far-field camera. The separation between the two resulting far-field spots is a measure of the effect the amplifiers have on beam pointing. Since the YAG was Q-switched, this measurement could be made just prior to firing the amplifiers and exactly at the gain peak, thereby providing a measure of the dynamic pointing that occurs during a shot. The result of these measurements indicated that the whole-beam steering in the horizontal direction due to firing of the disk amplifiers is less than 1 μrad. It is expected that no steering will occur in the vertical direction.

5. Laser Glass

In keeping with the philosophy of using proven, low-risk technologies, LHG-8 laser glass[23] was chosen as the active medium for the Upgrade. It is a well-characterized, athermal phosphate laser glass that provides a high cross section for stimulated emission, extremely low 1-μm absorption, and a reduced nonlinear index of refraction when compared with the silicate glasses. LHG-8 can be melted in production quantities while maintaining sufficient homogeneity and low particulate platinum content.

Nd-doped phosphate glasses are known[24] to be susceptible to shortening of the lifetime of the upper lasing level due to multiphonon de-excitiation by excess water in the glass melt. The minimum fluorescence lifetime is chosen to ensure that this effect is not a limiting factor in determining the amplifier performance.

The disk-cladding technology was developed at LLNL[11] utilizing a polymer bond to attach copper-doped LHG-8 glass to the disk edges in a stress-free manner. This cladding effectively reduces parasitic oscillations.

At the recommendation of LLE, the vendor utilized phase-shifting interferometry and polished-homogeneity-testing[25] technology to monitor the homogeneity of the production laser glass. This quality-control step assisted in the production of glass that exceeded the specifications for homogeneity. The specifications and work statements for the laser-glass procurement are contained in the design review package submitted for the KD3′. The selection and procurement of laser glass have been described elsewhere.[12]

6. Flash Lamps

The 217 laser amplifiers in the OMEGA Upgrade will require nearly 7,000 flash lamps. These units will be 19-mm-bore, 300-Torr, xenon flash lamps and will have arc lengths of 0.25, 1.32, and 0.3 m for the 20-cm SSA, 15-cm SSA, and rod amplifiers, respectively. Other than the arc length all features of the flash lamps are identical.

All of the OMEGA Upgrade flash lamps are water cooled, thus providing a number of advantages over air-cooled flash lamps: The lamps can be run at a higher explosion fraction. (This is the operational energy divided by the maximum energy a lamp can survive and not explode.) The Upgrade lamps are operated at 26%–34% explosion fraction, whereas air-cooled lamps are normally operated at 20%–25%. The blanket of deionized water used to cool the lamps has high resistivity, which eliminates electrical arcing. The water also provides mechanical support allowing the use of lower-cost, industry-standard, 1.5-mm-thick jackets rather than custom heavy-wall jackets favored on other laser systems. Lastly, water-cooled flash lamps increase the transfer of thermal energy out of the amplifier after a shot. Air-cooled lamps, which dissipate thermal energy by radiation, ultimately heat the laser glass after a shot; water cooling removes this heat without heating the laser glass.

Along with the visible light used to pump Nd lasers, xenon flash lamps produce large amounts of UV light. The solarization of phosphate laser glass when exposed to intense UV light is a problem in high-power-laser designs. In the design of prototype amplifiers for the OMEGA Upgrade, the desire to eliminate as much UV light as possible has led to the use of cerium-doped-quartz (CDQ) envelopes that absorb much of the UV radiation from the flash-lamp discharge. Recently, an additional attenuation of the UV radiation has been achieved using a new manufacturing process for the envelopes. The use of cerium-doped quartz and the new process for producing that quartz are the most significant improvements to these flash lamps relative to their predecessors.

Originally, CDQ for flash lamps was manufactured using a multistep process. Quartz was produced using an oxygen/hydrogen flame, resulting in solid quartz ingots from which tubing for flash lamps was drawn. In the new, single-step process the raw material is melted in a crucible, and tubing is drawn directly from the bottom of the crucible. This process reduces the OH content of the quartz that

produces a concomitant reduction in the UV transmission of the quartz. Shown in Fig. 56.39 are the transmission curves for CDQ manufactured by the two processes. Note the marked reduction in the UV transmission and the virtually unchanged transmission in the visible band for the single-step process.

Table 56.VII shows a comparison of a few key parameters for the two manufacturing processes. The first three attributes favorably impact the performance and design, i.e., lower OH content, lower cost, and better tolerances. The last three attributes are primarily cosmetic in nature and are permitted, to some extent, without compromising flash-lamp performance.

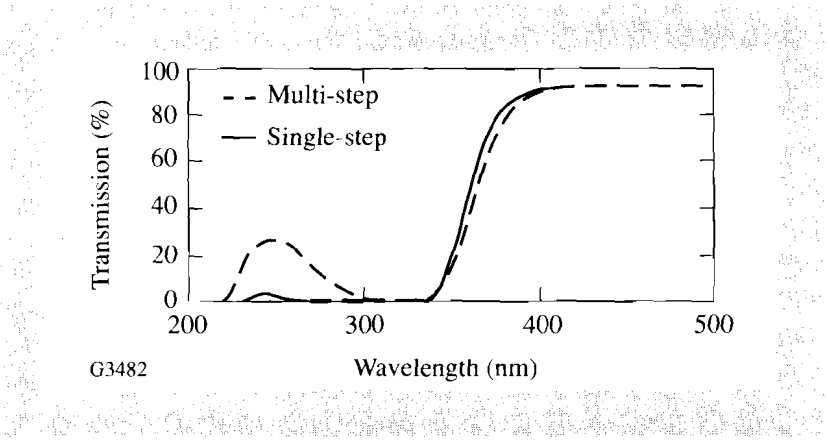

Fig. 56.39
The output spectrum of the xenon flash lamps with cerium-doped quartz envelopes made with a multistep process (dashed) and a single-step process (solid). The newer, single-step process reduces unwanted UV radiation in the 250-nm range.

Table 56.VII: Comparison of single and multistep processes for producing cerium-doped quartz.

Attribute	Single-step Process	Multistep Process
OH content	80 ppm as drawn, vacuum anneal to < 8	130–220 ppm
Cost	Lower	Higher
Outside diameter and wall tolerances (mm)	±0.22/±0.12	±0.40/±0.40
Bubble content	Some	Minimal
Air lines (elongated bubbles)	Some	Minimal
Die and mandrel marks	Some	None

This completes the description of the subsystems of the OMEGA Upgrade Project, from Laser Drivers through Disk Amplifiers. In subsequent issues of the LLE Review, we shall provide the remainder of subsystems described in the Executive Summary. Subsystems yet to be described include Power Conditioning, Controls, Optomechanical Systems (both laser and target area), and Major Structures.

ACKNOWLEDGMENT

This work was supported by the U.S. Department of Energy Office of Inertial Confinement Fusion under Cooperative Agreement No. DE-FC03-92SF19460, the University of Rochester, and the New York State Energy Research and Development Authority.

REFERENCES

1. J. E. Murray and W. H. Lowdermilk, J. Appl. Phys. **51**, 3548 (1980).

2. J. E. Murray and D. J. Kuizenga, Appl. Phys. Lett. **37**, 27 (1980).

3. E. W. Roschger and J. E. Balmer, Appl. Opt. **24**, 3110 (1985).

4. S. Skupsky, R. W. Short, T. Kessler, R. S. Craxton, S. Letzring, and J. M. Soures, J. Appl. Phys. **66**, 3456 (1989).

5. D. L. Brown, I. Will, W. Seka, and M. Tracy, "Large-Aperture Ring Amplifier with Gains in Excess of 40,000 and Several-Joule Output Capability," presented at CLEO '93, Baltimore, MD, 2–7 May 1993; M. D. Tracy, I. Will, C. K. Merle, R. G. Roides, K. Thorp, M. D. Skeldon, J. H. Kelly, and W. Seka, "Versatile Front-End Laser System for Laser-Fusion Drivers," to be presented at the 1993 OSA Annual Meeting, Toronto, Canada, 3–8 October 1993.

6. The code used is a greatly updated and enhanced version of the code ZAP originally written by Systems, Science and Software for the Naval Research Laboratory by J. H. Alexander, M. Troost, and J. E. Welch, ARPA order number 660, Contract number N00014-70-C-0341, 1971.

7. We are grateful for the cooperation of our colleagues at Lawrence Livermore National Laboratory, especially Dr. H. T. Powell, Dr. J. E. Murray, and Dr. A. T. Erlandson.

8. J. Boon, C. Danson, and M. Mead, "ϕ108 Disc Amplifier Cooling," Rutherford Appleton Laboratory Annual Report to the Laser Facility Committee RAL-85-0047 (1985), pp. A6.6–A6.12.

9. S. M. Yarema and J. E. Murray, Lawrence Livermore National Laboratory Laser Program Annual Report 1980, UCRL 50021-80 (1981), pp. 2-234–2-244.

10. Private communication from K. Moncur, KMS Fusion (1989).

11. C. R. Wolfe, H. G. Patton, and H. T. Powell, Lawrence Livermore National Laboratory Laser Program Annual Report 1986, UCRL 50021-86 (1987), pp. 4-14–4-59.

12. M. J. Shoup III, S. D. Jacobs, J. H. Kelly, C. T. Cotton, S. F. B. Morse, and S. A. Kumpan, in *Solid State Lasers III* (SPIE, Bellingham, WA, 1992), Vol. 1627, pp. 192–201.

13. K. Wantanabe, E. C. Y. Inn, and M. Zelikoff, J. Chem. Phys. **21**, 1026 (1953).

14. A. C. Erlandson, Lawrence Livermore National Laboratory Laser Program Annual Report 1985, UCRL 50021-85 (1986), pp. 7-18–7-25.

15. M. Zahn *et al.*, Proc. IEEE **74**, 1182 (1986).

16. General Electric Company, One Plastics Avenue, Pittsfield, MA 01201. Reference to a company or a product name does not imply approval or recommendation of the product by the University of Rochester or the U.S. Department of Energy.

17. Corning Glass Works, Corning, NY 14830. Reference to a company or a product name does not imply approval or recommendation of the product by the University of Rochester or the U.S. Department of Energy.

18. W. C. Young, *Roark's Formulas for Stress & Strain*, 6th ed. (McGraw-Hill, New York, 1989), Chap. 13, pp. 647–665.

19. L. M. Frantz and J. S. Nodvik, J. Appl. Phys. **34**, 2346 (1963).

20. J. H. Kelly, M. J. Shoup III, M. M. Tedrow, and K. Thorp, "Energy Transport in a Modern Disk Amplifier," in *Solid State Lasers III* (SPIE, Bellingham, WA, 1992), Vol. 1627, pp. 286–297.

21. J. M. Auerbach, N. C. Holmes, J. T. Hunt, and G. J. Linford, Appl. Opt. **18**, 2495 (1979).

22. S. M. Yarema and D. Milam, IEEE J. Quantum Electron. **QE-18**, 1941 (1982).

23. Hoya Optics, Inc., 3400 Edison Way, Fremont, CA 94538-6190. Reference to a company or a product name does not imply approval or recommendation of the product by the University of Rochester or the U.S. Department of Energy.

24. C. B. Layne, Ph.D. Thesis, University of California, Davis, 1975.

25. A. Chiayu and J. C. Wyant, Opt. Eng. **30**, 1399 (1991).